Final Report

for

NASA Contract NAS 9-12236

Apollo Particles and Fields Subsatellite

Magnetometer Experiment

(S-174)

Principal Investigator: Paul J. Coleman, Jr.

Co- Investigators: Christopher T. Russell
Gerald Schubert

Prepared by

Christopher T. Russell
Institute of Geophysics and Planetary Physics
University of California
Los Angeles, California 90024

for

Johnson Space Center
Houston, Texas 77058

IGPP Publication Number 1372-55

July 1974

Table of Contents

1. The Experiment

1.1 Instrument Description

The subsatellite magnetometer consists of two fluxgate sensors mounted orthogonally at the end of a 1.83-m boom and an electronics unit housed in the main body of the spacecraft. The two sensors are mounted one parallel and one perpendicular to the spin axis. On the Apollo 15 subsatellite there are two automatically selected dynamic ranges 0 to $\pm 50\gamma$ and 0 to $\pm 200\gamma$. These are called the high sensitivity and low sensitivity ranges, respectively. The resolution of each measurement is 0.4 to 1.6γ depending on range. There are three sampling rates referred to as telemetry store normal (TSN), telemetry store fast (TSF) and real time (RT). In the former two modes, the magnetometer measures the magnitude and phase of the magnetic field in the spin plane and the vector component along the spin axis. The sample rates are one vector every 24 seconds and every 12 seconds, respectively. The magnitude in the spin plane is measured by filtering the transverse magnetometer output about the spin frequency, rectifying and filtering this. The phase is obtained by measuring both the time of the positive going zero crossing of the magnetometer output and the time of the sun crossing. In eclipse, the sun crossing time is computed from a model of the eclipse spin up and from a knowledge of the spin frequency and phase during the sunlit portion of the orbit.

During real time operations, one sample of the spin plane output is returned every second and of the spin axis output every 2 seconds. Thus, there are about 5 samples of the spin plane signal per revolution. This signal is Fourier analyzed to obtain a magnitude and phase and referenced to the sun crossing time. Real time data are, of course, only obtained across the near side of the moon, whereas the recorded TSF and TSN data are available from both near and far sides. We note that the subsatellite did not store data while transmitting. Thus, there are gaps in the records every orbit when data were telemetered to earth. A summary of the magnetometer characteristics is given in Table 1. The only significant difference between the Apollo 15 and 16 magnetometers is an increase by a factor of 2 in the sensitivity of the Apollo 16 magnetometer increasing the resolution to 0.2 and 0.8γ and decreasing the range to $\pm$25γ and $\pm$100γ for high and low sensitivity ranges, respectively.

1.2 Operating History

The Apollo 15 subsatellite was launched on August 4, 1971. A failure in the telemetry system after seven months of operation prevented further transmission of data from most of the magnetometer outputs although the magnetometer continued to operate normally. The Apollo 16 subsatellite was launched on April 24, 1972, into an approximately circular orbit at an altitude of 100 km, having an orbital period of close to 2 hours. Due to the decision not to perform a shaping burn prior to jettisoning the subsatellite, the Apollo 16 subsatellite crashed into the moon after 34 days in lunar orbit.

TABLE I.- APOLLO SUBSATELLITE MAGNETOMETER SPECIFICATIONS

Characteristic	Specification
Type	Second-harmonic, saturable core fluxgate
Sensor configuration	Two sensors, one sensor parallel B_P and one perpendicular B_T to the satellite-spin axis
Mounting	Sensor unit at end of 1.83-m boom; electronics unit in spacecraft body
Automatically selected dynamic ranges, γ	0 to ±50 at higher sensitivity, 0 to ±200 at lower sensitivity
Resolutions, γ	0.4 and 1.6, depending on range
Sampling rates:	
Real time	B_P every 2 seconds, B_T every second
High-rate storage	B_P and B_T magnitude and B_T phase once every 12 seconds
Low-rate storage	B_P and B_T magnitude and B_T phase once every 24 seconds
Power, W	0.70
Weight:	
Electronics unit, kg	≈0.8
Sensor unit, kg	≈0.2
Size:	
Electronics unit, cm	27.9 by 15.9 by 3.8
Sensor unit, cm	1.5 (diameter) by 7.6
Operating temperature range, °K	344 to 172

During this period the magnetometers operated normally. The minimum correlation technique of Hedgecock was used to measure sensor drift of the parallel axis. The drift rate was well within the range expected. Table 2 gives the offsets for each lunation of Apollo 15. These numbers should be added to the values presently on the plots and tapes which were obtained from the preliminary calibration. Corrected values were used in the Apollo 16 processing.

The orientation of the spin axis of the subsatellite was determined from the variation of the sun elevation angle with time during the first 30 days after launch. On Apollo 15 the predicted variation of this angle and the measured variation followed each other almost exactly until December 1971. Thereafter, measurable deviation occurred amounting to 1^{o} in February 1972.

Table 2 Magnetometer Offsets

Duration	Orbit Number	Offset
1	1 - 378	0.27γ
2	379 - 732	0.05
3	733 - 1086	-0.17
4	1087 - 1440	-0.38
5	1441 - 1784	-0.60
6	1785 - END	-0.81

2. The Data

Two types of data are relevant to this experiment: the support data and the observations. The support data consists of orbital information generated to relate the measurements to lunar position and the observations consist of magnetic field data and engineering parameters telemetered from the spacecraft. In this section we describe the data as it has been sent to the National Space Science Data Center.

2.1 Orbit Data

Three different displays of orbit data have been made plus one tape. These were all created at the Manned Spacecraft Center under the supervision of W. Wollenhaupt. The three orbit plots are altitude versus time, selenographic longitude versus latitude, and the ecliptic projection of the earth-moon system.

2.1.1 Altitude versus time

This plot shows altitude versus time for one orbit, but includes information on up to six consecutive orbits. At the top of the plot are the orbit number, the orbit start time (hours and minutes, day/month/year), the perilune time and altitude (km), the apolune time and altitude, and the time of sunrise and sunset. The plot includes two vertical shaded bars marking sunset and sunrise at the subsatellite. Time grids below the plot permit the use of this graph for up to six consecutive orbits. However, these grids may be up to four minutes off. Figure 1 shows a sample plot.

APOLLO 15 SUBSATELLITE

CALCULATED 8/04/71 TRACKING ORBIT = 1 PROCESSED 3/11/72

ORBIT	START		PERILUNE		APOLUNE		SUNRISE	SUNSET
1	2019	8/04/71	2041	100.4	2141	138.4	2141	2055
2	2219	8/04/71	2241	100.6	2340	138.1	2340	2254
3	18	8/05/71	40	100.9	140	137.8	140	54

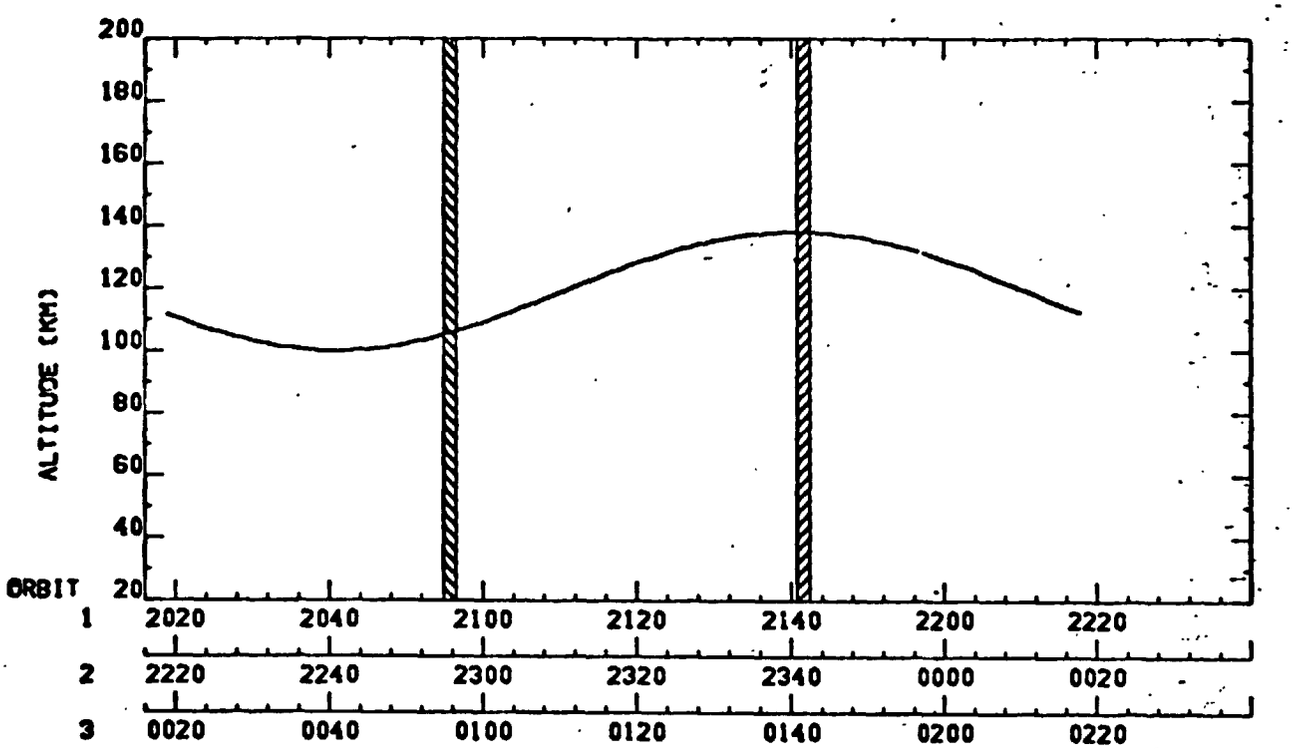

UNIVERSAL TIME

Figure 1

2.1.2 Latitude versus Longitude

This plot shows the track of the satellite across the lunar surface in selenographic coordinates. We note that the vertical and horizontal scale are different by a factor of two. The points of sunrise and sunset at the subsatellite are indicated by shaded vertical bars. Perilune and apolune are marked on the orbit track with an 'X' and labelled with P and A, respectively. The subsolar point is similarly marked with an 'X' and labelled with an S. The location of the Apollo 15 ALSEP is similarly shown and encircled by an ellipse showing the area within 15^{o} of the ALSEP site. Underneath the plot are given orbit numbers, perilune and apolune times. Figure 2 shows a sample plot.

2.1.3 Earth-moon system plots

This plot gives the ecliptic plane projection of the earth-moon system and includes the expected position of the magnetopause and bow shock. One point is given per orbit. Distances are labelled in earth radii. Figure 3 shows a sample plot.

2.1.4 Magnetic tape

The orbit tape contains position and orientation information which changes slowly in a header record once per orbit and rapidly changing positional data every minute in a data record (one record per minute). The format of this tape is given in Table 3.

APOLLO 15 SUBSATELLITE SELENOGRAPHIC COORDINATES

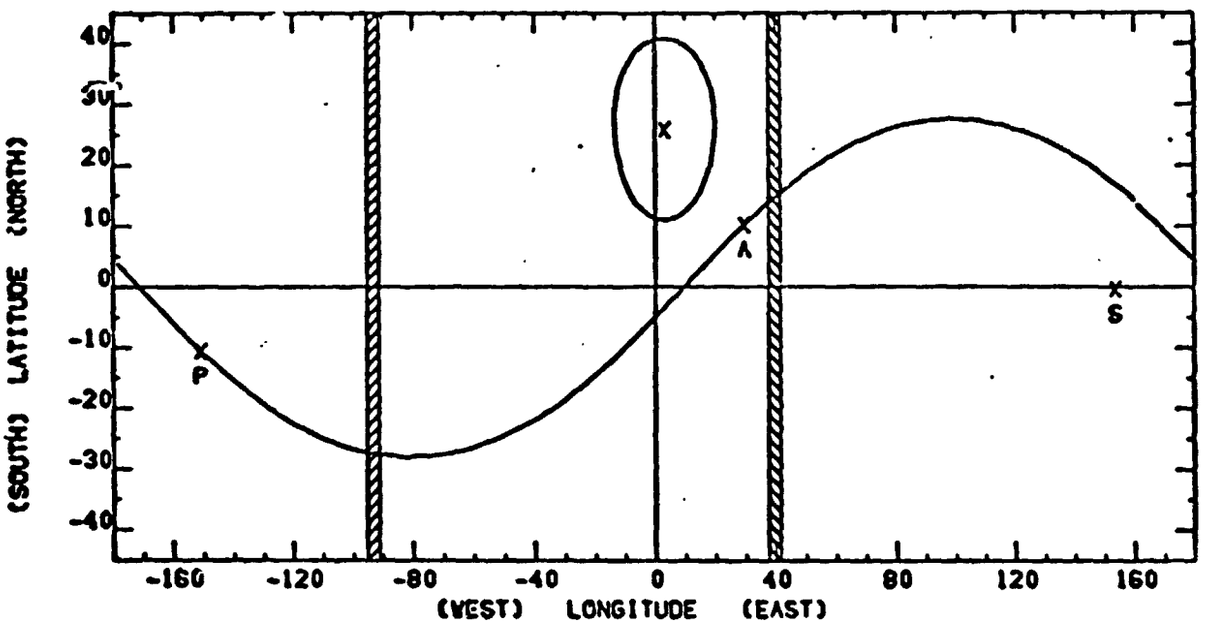

ORBIT	2002	2003	2004	2005	2006	2007
PERILUNE	542	742	942	1142	1342	1541
APOLUNE	442	642	842	1042	1242	1442

START DAY-FIRST ORBIT 1/18/72 CALCULATED 1/18/72 PROCESSED 3/04/72
TRACKING ORBIT - 2013

PAGE [illegible]

Figure 2

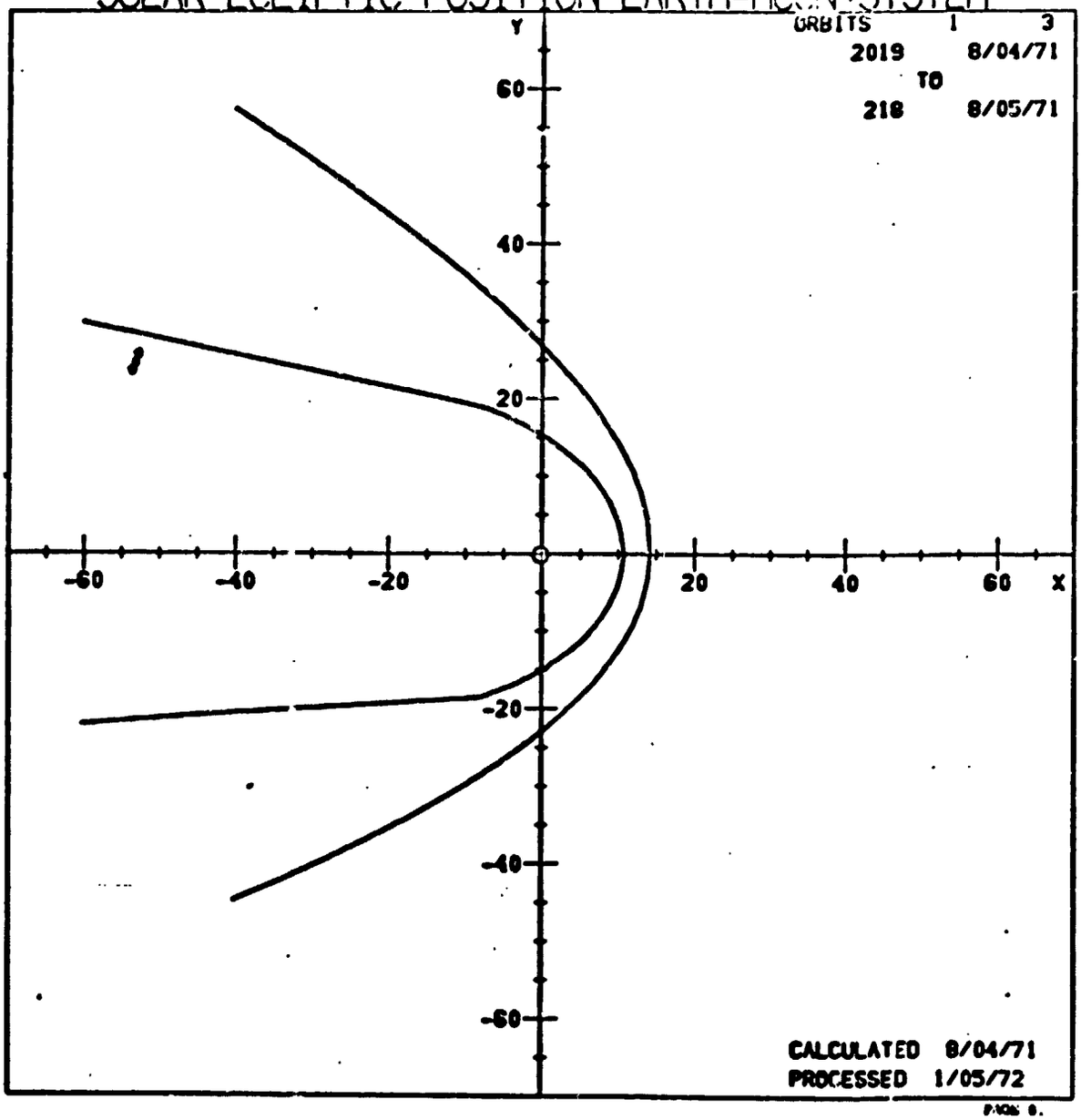
SOLAR ECLIPTIC POSITION EARTH-MOON SYSTEM
ORBITS 1 3
2019 8/04/71
TO
218 8/05/71
Y
60
40
20
-20
-40
-60
-60
-40
-20
20
40
60
X
CALCULATED 8/04/71
PROCESSED 1/05/72

Figure 3

Table 3

Orbit Tape Contents

Header Record (Record 1)

Words 1-4 Integer, words 5 on Real.

1. Number of orbit on tape

2. Orbit number

3/4 Date calculated/processed

5/6 Altitude of perilune/apolune

7/8 Day of year of orbit start/year mod. 1900

9 Start time (seconds)

10 Number of poirts (records) in orbit

11/12 Time of perilune/apolune

13/14 Sunset time (start/stop)

15/16 Sunrise time (start/stop)

17/18 Earthrise/earthset times

19 End time of orbit

Transformation matrices of form A11 A12 A13, A21 A22 A23, A31 A32 A33

20-28	GEI to GSE	101-109	GEI to SG
29-37	GEI to GSM	110-118	SG to SSE
38-46	GEI to GSEQ	119-127	SG to SSEQ
47-55	GSM to GSE	128-136	SG to GSM
56-64	GSM to GSEQ	137-145	S/C to SSE
65-73	GSE to GSEQ	146-154	S/C to SSEQ
74-82	GEI to SSE	155-63	S/C to GSM
83-91	GEI to SSEQ	164-172	S/C to GSE
92-100	SSE to SSEQ	173-181	S/C to SG

Table 3 (continued)

GEI = geocentric equatorial inertial coordinates

GSE = geocentric solar eclipitic

GSM = geocentric solar magnetospheric

GSEQ = geocentric solar equatorial

SSE = selenocentric solar ecliptic

SG = selenographic

S/C = spacecraft coordinate

Data Record - Repeated N times - All real

1/2 Day of year/year mod. 1900

3 Seconds of day

4/5 Earth-sun/earth-moon distances

6/7 Sun-moon/subsatellite-moon distances

8-10 Unit vector to sun GEI

11-13 Unit vector to moon GEI

14-16 Unit vector parallel PFS spin axis GEI

17-19 Unit vector parallel earth's dipole GEI

20-22 Unit vector to earth SSE

23-25 Unit vector to subsatellite SSE

26-28 Unit vector parallel to PFS spin axis SSE

29-31 Unit vector to subsatellite SG

32-34 Unit vector to earth SG

35-37 Unit vector to sun SG

38-40 Unit vector parallel to PFS spin axis SG

41 Altitude of PFS

2.2 Magnetometer data

Two microfilm reels of data and one magnetic tape have been produced in preliminary processing of the data. The first reel contains two plots consisting of magnetometer measurements on the A plot and engineering data on the B plot. The second reel contains a computer listing of 192 second averages of the data. The magnetic tape contains 24 second averages of the data.

2.2.1 The A Plot

This plot shows the B_x, B_y, B_z components and B_t (total field) in spacecraft coordinates versus time for one orbit. The orbit start time is defined here and in the orbit data to be the time of the crossing of the lunar noon meridian. Spacecraft coordinates have X and Y in the spin plane with X along the projection of the earth-sun line in the spin plane and Y roughly antiparallel the direction of planetary motion. The Z direction is chosen to be parallel to the spin axis and points northward relative to the ecliptic plane. At launch the spin axes of both the Apollo 15 and 16 subsatellites were close to perpendicular to the ecliptic. Thus initially the data were returned in essentially solar ecliptic coordinates. Time on the horizontal scale is given in terms of day of year (Jan 1-1), hour and minute. No sensor drift corrections have been applied to these data. Note that the scale of this plot varies to keep the data on scale. Figure 4 shows a sample plot.

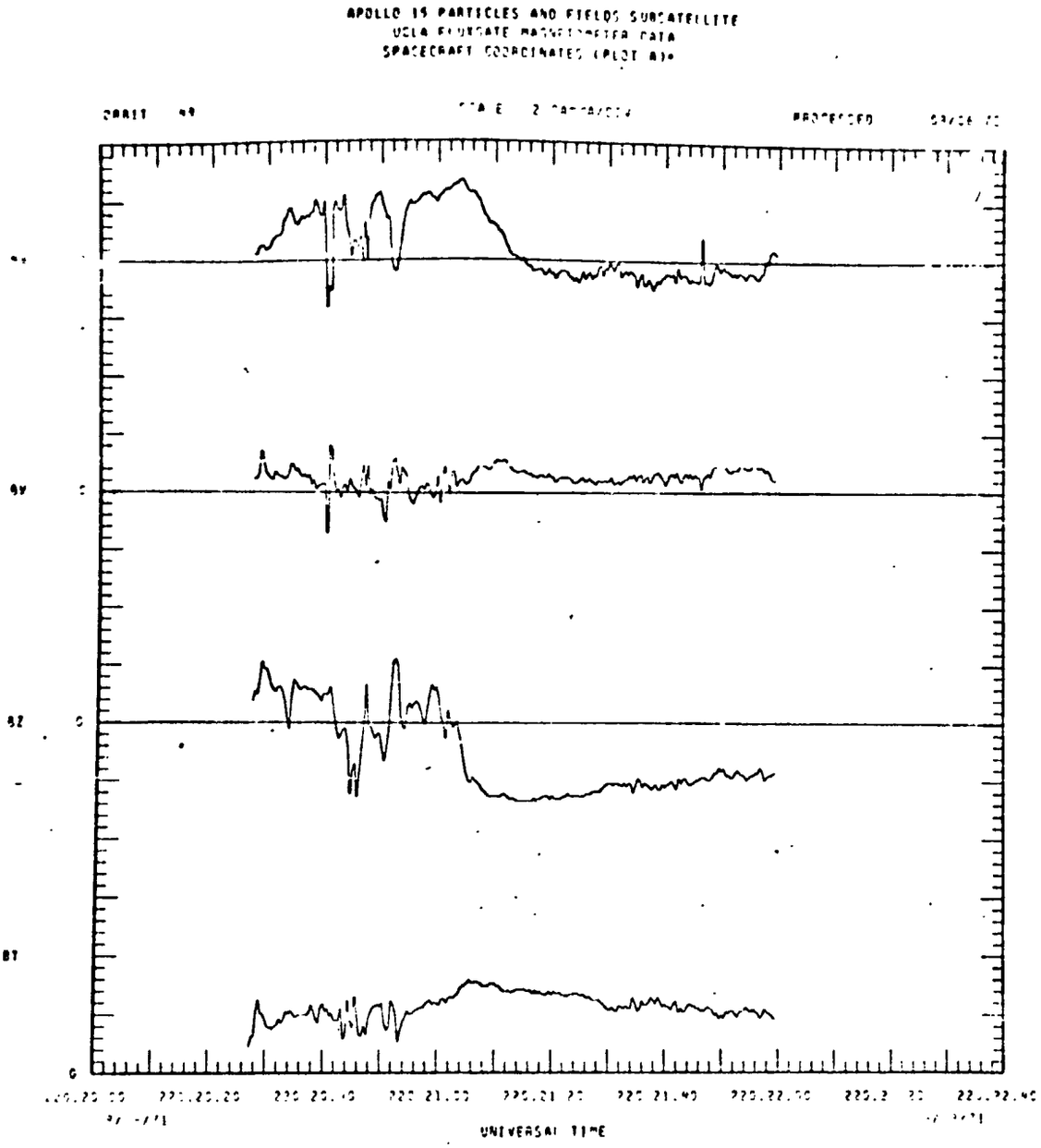
APOLLO 15 PARTICLES AND FIELDS SUBSATELLITE
UCLA FLUXGATE MAGNETOMETER DATA
SPACECRAFT COORDINATES (PLOT A)
BV
BZ
BT
UNIVERSAL TIME

Figure 4

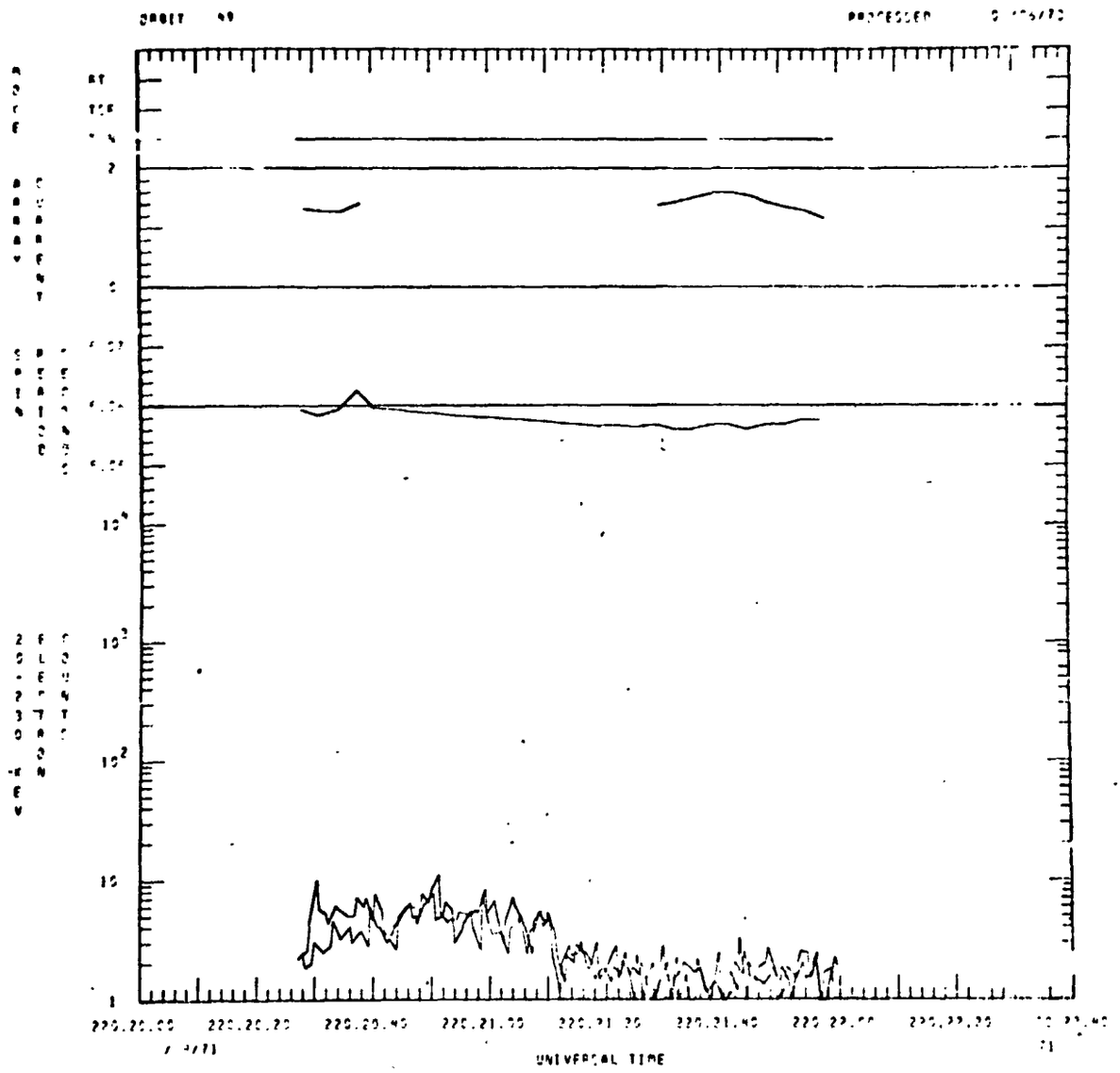
APOLLO 15 PARTICLES AND FIELDS SUBSATELLITE
UCLA FLUXGATE MAGNETOMETER DATA
SPACECRAFT COORDINATES (PIOT 03)
ORBIT 49
PROCESSED
UNIVERSAL TIME

Figure 5

2.2.2 The B plot

The second plot contains relevant engineering and processing data and some data from the Berkeley particle experiment. The top line shows the telemetry mode TSN, TSF or RT. The second shows the array current in amps. The third shows the spin period in seconds. This is measured in sunlight and predicted in eclipse. Finally, on the bottom plotted on the same scale are Berkeley particle counts per accumulation period for the shielded and unshielded detectors. Figure 5 shows a sample plot.

2.2.3 The Printout

The microfilm reel containing the printout of the data first contains data and tables generated during the processing of the data. The printouts which follow are 192 second averages of the data (192 seconds is the basic repetition cycle of the data system). The data given are:

Day of year (Jan. 1=1)

Month/day

Elapsed time on spacecraft clock (1 tick=16 sec)

B_X, B_y, B_z, B_T (spacecraft coordinates, in gammas)

Open counts (Berkeley data)

Shielded counts (Berkeley data)

Sun elevation angle (degrees)

Spin period (seconds)

Spin count (from sun pulse or magnetometer pulse)

Magnetometer temperature (^oF)

Battery temperature (^oF)

Battery voltage (volts)

Battery current (amps)

Array current (amps)

Reference voltage of magnetometer (volts)

Flag 1 I Satellite ID (1=Apollo 15)

F Data format (0=Store mode, 1=Real time)

M Automatic/manual (0=Manual mode)

C Calibration (1=On)

T Transverse range (1=low sensitivity)

P Parallel range (1=low sensitivity)

Flag 2 not used (repeats elapsed time fine). Figure 6 shows a sample plot.

2.2.4 Magnetic tape

The magnetic tape contains magnetic field data every 24 seconds and associated engineering data every 192 seconds. Its format is given in Table 4.

Figure 6

PARTICLES AND FIELDS MAGNETOMETER DATA APOLLO 15 ----------ORBIT 49---------- PROCESSED 08/06/73

DAY	MN/DY	HRMN:SC	EL.TIME C	EL.TIME F	MAGNETIC FIELD (GAMMAS) BX	BY	BZ	BT	PARTICLE COUNTS OPEN	SHIELDED	SUN ANG	SPIN PER.	SPIN COUNT	MAG TEMP	BATT TEMP	BATT VOLT	BATT CURR	ARRAY CRUR	REF VOLT	FLAG1 IFMCTP	FLAG2 RTP
220	8/ 8	2027:21	83193		2.11	3.75	7.30	8.58	2	-2	-.3	5.059	170	67.8	70.2	16.8	.57	1.31	2.50	111000	193
220	8/ 8	2030:33	83206		5.44	2.75	4.95	8.21	6	-3	-.3	5.058	208	67.8	70.7	16.8	.65	1.27	2.50	111000	205
220	8/ 8	2033:45	83217		7.27	3.43	5.20	10.03	5	-3	-.3	5.059	246	67.8	70.7	16.8	.67	1.27	2.50	111000	217
220	8/ 8	2036:57	83229		8.61	1.53	5.05	10.07	6	-3	-.5	5.062	29	67.8	71.1	16.8	.65	1.42	2.50	111000	229
220	8/ 8	2040:09	83241		3.05	1.27	1.06	9.30	5	-3	-.5	5.059	65	67.8	71.1	14.5	-.69	.00	2.50	111000	241
220	8/ 8	2043:21	83253		4.15	.84	-6.92	9.34	4	-4	.0	5.059	103	67.8	71.6	14.3	-.70	.00	2.50	111000	253
220	8/ 8	2046:33	84 9		6.69	.91	-.75	8.61	5	-5	.0	5.059	142	67.3	71.6	14.2	-.70	.00	2.50	111000	9
220	8/ 8	2049:45	84 21		4.79	.84	.84	10.24	7	-5	.0	5.059	180	67.3	71.6	14.0	-.70	.00	2.50	111000	21
220	8/ 8	2052:57	84 33		4.95	.96	2.57	8.38	4	-4	.0	5.058	218	66.8	71.6	14.0	-.70	.00	2.50	111000	33
220	8/ 8	2056:09	84 45		10.68	.53	2.95	11.28	5	-4	.0	5.058	0	66.2	71.1	13.8	-.72	.00	2.50	111000	45
220	8/ 8	2059:21	84 57		11.17	1.72	1.95	12.02	6	-3	.0	5.058	38	65.7	71.1	13.8	-.72	.00	2.50	111000	57
220	8/ 9	2102:33	84 69		12.47	2.02	-4.04	13.95	5	-3	.0	5.058	76	65.7	71.1	13.6	-.72	.00	2.50	111000	69
220	8/ 8	2105:45	84 81		9.42	4.21	-10.24	15.22	3	-3	.0	5.057	114	65.2	70.7	13.6	-.73	.00	2.50	111000	81
220	8/ 8	2108:57	84 93		5.05	5.30	-12.65	14.65	4	-3	.0	5.057	152	64.7	70.7	13.5	-.73	.00	2.50	111000	93
220	8/ 8	2112:09	84105		.68	3.95	-13.30	13.91	2	-2	.0	5.057	190	64.2	70.2	13.4	-.73	.00	2.50	111000	105
220	8/ 8	2115:21	84117		-1.38	3.11	-13.41	13.84	2	-2	.0	5.057	228	64.2	69.7	13.3	-.75	.00	2.50	111000	117
220	8/ 8	2118:33	84129		-2.27	2.62	-12.97	13.44	2	-1	.0	5.057	10	63.7	69.2	13.3	-.75	.00	2.50	111000	129
220	8/ 8	2121:45	84141		-2.46	2.24	-12.79	13.28	2	-1	.0	5.056	48	63.2	68.7	13.3	-.75	.00	2.50	111000	141
220	8/ 8	2124:57	84153		-2.58	2.10	-12.44	12.89	1	-1	.0	5.056	86	62.7	68.7	16.8	.30	.00	2.50	111000	153
220	8/ 8	2128:09	84165		-1.32	2.03	-11.15	11.43	1	-1	-.5	5.057	123	62.7	68.2	16.6	.68	1.34	2.50	111000	165
220	8/ 8	2131:21	84177		-1.48	2.19	-10.56	10.95	1	-1	-.3	5.056	161	62.7	67.7	16.5	.85	1.43	2.50	111000	177
220	8/ 8	2134:33	84189		-3.28	2.46	-10.75	11.58	1	-1	-.3	5.056	199	62.2	67.3	16.5	.79	1.51	2.50	111000	189
220	8/ 8	2137:45	84201		-3.24	2.43	-11.20	12.00	1	-1	-.3	5.057	237	62.7	66.8	16.6	.74	1.58	2.50	111000	201
220	8/ 8	2140:57	84213		-2.42	2.34	-10.25	10.94	1	-1	-.3	5.057	19	62.7	66.8	16.6	.77	1.59	2.50	111000	213
220	8/ 8	2144:09	84225		-2.41	2.43	-10.14	11.03	1	-1	-.3	5.056	57	62.7	66.3	16.8	.36	1.53	2.50	111000	225
220	8/ 8	2147:21	84237		-2.02	3.90	-9.14	10.24	1	-1	-.1	5.057	95	63.2	66.3	16.7	.82	1.41	2.50	111000	237
220	8/ 8	2150:33	84249		-1.95	4.12	-8.93	10.05	1	-1	-.3	5.057	133	63.2	66.3	16.6	.70	1.33	2.50	111000	249
220	8/ 9	2153:45	85 5		-2.49	4.33	-9.22	10.52	1	-1	-.3	5.058	171	63.7	66.3	16.6	.52	1.27	2.50	111000	5
220	8/ 8	2156:57	85 17		.21	3.35	-8.96	9.73	1	-1	-.1	5.058	209	64.2	66.3	16.6	.46	1.16	2.50	111000	17

DAY	MN/DY	HRMN:SC	EL.TIME C	EL.TIME F	MAGNETIC FIELD (GAMMAS) BX	BY	BZ	BT	PARTICLE COUNTS OPEN	SHIELDED	SUN ANG	SPIN PER.	SPIN COUNT	MAG TEMP	BATT TEMP	BATT VOLT	BATT CURR	ARRAY CRUR	REF VOLT	FLAG1 IFMCTP	FLAG2 RTP

SUBJECT: LUNAR SUBSATELLITE MAGNETOMETER DATA REDUCTION PROGRAM (SSMAGE)
PHASE 3 DATA TAPE FORMAT

PHYSICAL DESCRIPTION OF THE TAPE*
A. PARITY: ODD
B. DENSITY: 800 BPI
C. WORD LENGTH: 36 BITS
D. WORD MODES USED
   1. INTEGER
   2. FLOATING POINT
   3. FIELDATA
E. FORMAT

RECORD NO.	NO. OF WORDS	MODE	ARRAY	DESCRIPTION
1	5	MIXED		PROCESSING DATE AND ROUTINE VERSION
2	100	INTEGER	ORBIT(100)	Lunar orbit numbers for data contained on this tape
3	100	INTEGER	NOON(100)	Lunar noon meridians associated with the beginning of each of the above orbits
4	100	INTEGER	ECLIPSE(100)	Lunar eclipse time associated with the above orbits
5	100	INTEGER	SUNRIS(100)	Lunar sunrise time associated with the above orbits
6	200	INTEGER	ECL(100,2)	Lunar eclipse intervals (start and stop times) found from the data (last subscript denotes start or stop)
7	200	INTEGER	SUN(100,2)	Lunar sunlight intervals found from the data
8	200	INTEGER	ASUN(100,2)	Lunar sunlight intervals prior to lunar eclipse found from the data associated with the above orbits

WORD	MODE	DESCRIPTION
1	FIELDATA	Date processed "DDMMYY"
2	FIELDATA	Time of day processed "HHMMSS"
3	INTEGER	Routine version number
4	FIELDATA	Routine version generation date "DDMMYY"
5	FIELDATA	Routine version generation time of day "HHMMSS"

*Written on Univac 1108

8/10/72

RECORD NO.	NO. OF WORDS	MODE	ARRAY	DESCRIPTION
9	200	INTEGER	NITE(100,2)	Lunar eclipse intervals found from the data associated with the above orbits
10	200	INTEGER	MSUN(100,2)	Lunar sunlight intervals after lunar eclipse found from the data associated with the above orbits
11	200	INTEGER	BN(100,2)	TSN data intervals found from the data
12	200	INTEGER	TSF(100,2)	TSF data intervals found from the data
13	200	INTEGER	RT(100,2)	Real time data intervals found from the data Note: All the above times are integer milliseconds (a) 1 Day = 86,400,000 milliseconds (b) 1 Hour = 3,600,000 milliseconds (c) 1 Minute = 60,000 milliseconds
14-N	560	MIXED	BUF(560)	24 second average data Note: The BUF array is described in terms of (a) 8 words per frame (b) 8 frames per data cycle (c) 16 extra words per data cycle (d) 80 total words per data cycle (e) 7 data cycles per record (f) ~~196~~ 192 seconds per data cycle SEE DESCRIPTION OF A DATA CYCLE BELOW

N - is the total number of records on the tape and is followed by 2 1108 software end-of-file marks, i.e., one word records containing an octal 17 in the 6 most significant bits and the remaining 30 least significant bits are zero.

8/10/72

DATA CYCLE DESCRIPTION

1 Data Cycle is 80 words. It is considered as an array dimensioned 8 by 10.

Then for DATCYC(8,10) or DATCYC(I,J):

1. I implies A_I for I = 1 to I = 8.
2. J implies frame of A_1 for J = 1 to J = 8.
3. J is meaningless for A_I for J = 9 to J = 10, but the B_K data is contained in these cells.
   a. K takes on values 1 through 16.
   b. K = I + (J-9)*8 for I = 1 to I = 8, J = 9 and J = 10.

Graphically, DATCYC(8,10) looks as follows:

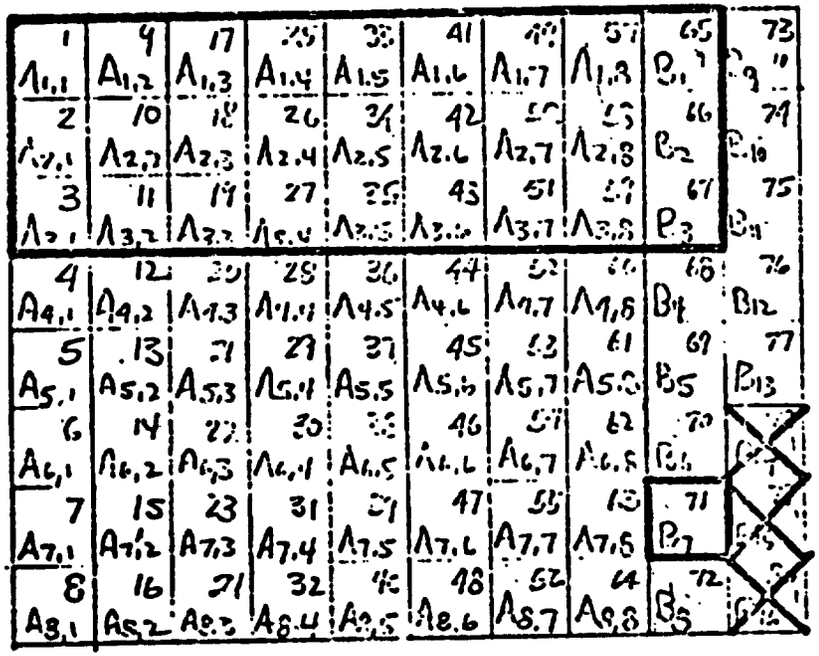

Integer Cells

Floating Point Cells

Cells Not Used

8/10/72

From the above chart it is evident that:

(1) ((A(I,J),I=1,3),J=1,8) are integer numbers

(2) ((A(I,J),I=4,8),J=1,8) are floating point numbers

(3) (B(K),K=1,3) and B(7) are integer numbers

(4) (B(K),K=4,6) and (B(K),K=8,13) are floating point numbers

(5) (B(K),K=14,16) are cells not used.

Quantity	Description
A(1,J)	Time (days)
A(2,J)	Time(milliseconds of day)
A(3,J)	Flag
A(4,J)	Transverse Field (Gammas)
A(5,J)	Parallel Field (Gammas)
A(6,J)	Sun Pulse Delay (seconds)
A(7,J)	Magnetometer Time Delay (seconds)
A(8,J)	Particle Counts
B(1)	Elapsed time coarse
B(2)	Elapsed time fine
B(3)	Flag
B(4)	Sun Elevation Angle (Degrees)
B(5)	Spin Period
B(6)	Sector Period
B(7)	Spin Count
B(8)	Magnetometer Temperature (^{o}F)
B(9)	Battery Temperature (^{o}F)
B(10)	Battery Current (amps)
B(11)	Battery Voltage (volts)
B(12)	Array Current (amps)
B(13)	Reference Voltage (volts)

3. Summary of Results

3.1 Lunar Magnetic Field

The earliest data clearly showed the evidence of fossil lunar magnetism during the portion of each lunation when the moon was in the geomagnetic tail (1-1, 1-2).* These lunar fields were most evident over the farside highlands. Preliminary quick look data were used to construct a contour map of the lunar contributions to the transverse magnitude choosing an arbitrary zero level near the crater Van de Graaff (1-3, 1-4). The Van de Graaff region at about 170°E and 20°S has the strongest fields encountered along the Apollo 15 subsatellite orbit track and was the first to be examined with low altitude data (1-4, 1-5). These data revealed that the magcon was not centered on either the crater Van de Graaff or the crater Aitken. At 67 km the field over Van de Graaff was about 2.5γ. The launch of the Apollo 16 subsatellite provided data at all altitudes from 200 km down to the lunar surface. Below 20 km fields up to 50γ were observed (1-6, 1-7).

The receipt of data on digital magnetic tapes permitted routine large scale mapping of the vector magnetic field in lunar coordinates. Maps of the radial component of the lunar field over the Apollo 15 orbit track have been created (1-8). High resolution maps over the Van de Graaff region at two

*Numbers refer to papers listed in the bibliography in section 4.

altitudes, 67 and 130 km permitted a scale size of 83 km to be deduced (1-8). Three component vector maps over this region have also been produced (1-12). Recently a new technique for observing these magnetic features has been developed by the Berkeley group (2-2), both confirming and extending these results.

Fourier analysis of the radial and tangential components of the field has permitted a limit of 2×10^{18} Γ-cm^3 to be placed on the present day dipole moment in the subsatellite orbit plane (1-11, 1-12). However, since the possibility was raised that the moon has a significant induced dipole moment, we re-examined the dipole field measurement taking care to remove and measure induced effects. This lowered the measured permanent moment in the orbit plane to less than $1.3 \times 10^{18}\Gamma$-cm^3 and gave an induced moment of $-6.3 \times 10^{22}\Gamma$-cm^3 per Gauss of external field (1-13, 1-14). The fact that this is negative indicates the presence of a weak lunar ionosphere. Analysis of Apollo 16 data confirms this result (1-16). Further, the addition of the Apollo 16 data taken around a belt with a significantly different lunar pole permits the calculation of all three components of the lunar dipole moment. The total permanent moment is certainly less than $10^{19}\Gamma$-cm^3 and probably much less. The present lunar dipole field is so low that it is unlikely that the moon ever had a large magnetic dipole moon as sometimes suggested.

Finally, with the availability of the Apollo 16 data maps of the fine scale lunar field have been created over all the subsatellite orbit tracks while they were in the geomagnetic tail. These maps have been submitted for publication in the Proceedings of the Fifth Lunar Science Conference.

3.2 The Solar Wind Interaction with the Moon

The previously known enhancement in the field strength on the antisolar side of the moon, when the moon is in the solar wind, known as the diamagnetic cavity, is also seen at the 100 km altitude of the subsatellite (1-1, 1-2). Also observed are the dips in field strength adjacent to the cavity which are presumed to occur because of the expansion of the solar wind flow into the cavity. One dominant feature of the interaction is the frequent increases in field strength just in front of the terminator. While these features were previously reported on Explorer 35, they are much larger at the low altitude of the subsatellite. These have previously been termed limb shocks or penumbral increases. However, we use the more conservative term, limb compression. They are definitely correlated with the appearance of certain regions at the limbs (1-3, 1-5, 1-6, 1-7). The property of the lunar surface that appears to be responsible for the deflection of the solar wind leading to a limb compression is the lunar remanent magnetic field (1-8, 1-12). On the other hand, the occurrence rate is also a function of the orientation of the interplanetary magnetic

field similar to the dependence of the structure of the earth's bow shock on the interplanetary field orientation (3-16).

3.3 The Transfer Function of the Moon

The region of the lunar limbs is usually disturbed even when limb compressions are absent (1-1, 1-2). However, comparisons with Explorer 35 magnetometer measurements show that the field is often undisturbed by the presence of the moon over much of the subsolar hemisphere (1-11, 1-12, 1-17, 1-18). Thus, the subsatellite magnetometer at times could be used as a measure of the input wave spectrum to the moon. On the other hand when the subsatellite is in the diamagnetic cavity, it is responsive to both the solar wind input and the scattered spectrum.

3.4 The Plasma Sheet Interaction with the Moon

When the moon is in the plasma sheet the average magnetic field as a function of selenocentric solar ecliptic longitude ressembles that in the solar wind but the enhancement is on the earthward side (1-17, 1-18). Further, the transfer function on the dayside (earthward side) ressembles that of the lunar cavity when the moon is in the solar wind. This suggests there is an earthward flow of plasma on the average in the plasma sheet at the lunar distance (1-15).

1. Published papers in which the subsatellite magnetometer data played a primary role.

1-1. Coleman, P.J., Jr., G. Schubert, C.T. Russell, L.R. Sharp The particles and fields subsatellite magnetometer experiment, in Apollo 15 Preliminary Science Report, NASA SP-289, 1972.

1-2. Coleman, P.J., Jr., G. Schubert, C.T. Russell, and L.R. Sharp, Satellite measurements of the Moon's Magnetic Field: A Preliminary report, The Moon, 4, 419, 1972.

1-3. Coleman, P.J., Jr., B.R. Lichtenstein, C.T. Russell, L.R. Sharp and G. Schubert, Magnetic fields near the moon, in Proceedings of the Third Lunar Science Conference, Vol. 3, 2271-2286, MIT Press, Cambridge, Mass., 1972.

1-4. Coleman, P.J., Jr., C.T. Russell, L.R. Sharp and G. Schubert, Preliminary mapping of the lunar magnetic field, Physics of Earth and Planetary Interiors, 6, 167-174, 1972.

1-5. Russell, C.T., P.J. Coleman, Jr., B.R. Lichtenstein, G. Schubert and L.R. Sharp, Surface and orbital results from Apollo 15, Space Research XIII, 951-960, 1972.

1-6. Coleman, P.J., Jr., B.R. Lichtenstein, C.T. Russell, G. Schubert and L.R. Sharp, The particles and fields subsatellite magnetometer experiment, in Apollo 16 Preliminary Science Report, NASA SP-315, 23-1 to 23-13, 1972.

1-7. Lichtenstein, B.R., C.T. Russell and P.J. Coleman, Jr., Magnetic measurements of the solar wind interaction with the moon, in the Proceedings of the Symposium on Photon and Particle Interactions with Surfaces in Space, Noordwijk, Holland,p. 471, D. Reidel Publ. Co., 1974.

1-8. Sharp, L.R., P.J. Coleman, Jr., B.R. Lichtenstein, C.T. Russell and G. Schubert, Orbital mapping of the lunar magnetic field, The Moon, 7, 322, 1973.

1-9. Russell, C.T., P.J. Coleman, Jr., B.R. Lichtenstein, G. Schubert and L.R. Sharp, Lunar magnetic fields, (extended abstract) Proceedings of Conference on Geophysical and Geochemical Exploration of the Moon and Planets, Lunar Science Institute, 1973.

1-10. Schubert, G., B.R. Lichtenstein, P.J. Coleman, Jr., and C.T. Russell, Simultaneous observations of transient events by the Explorer 35 and Apollo 15 subsatellite magnetometers: Implications for lunar electrical conductivity studies, J. Geophys. Res., 79, 2007, 1974.

1-11. Russell, C.T., P.J. Coleman, Jr., B.R. Lichtenstein, G. Schubert and L.R. Sharp, Subsatellite measurements of the lunar magnetic field, in Proceedings of the Fourth Lunar Science Conference, 2833, Pergamon Press, 1973.

1-12. Russell, C.T., P.J. Coleman, Jr., B.R. Lichtenstein, G. Schubert and L.R. Sharp, Apollo 15 and 16 subsatellite measurements of the lunar magnetic field, Space Research XIV, 629, 1974.

1-13. Russell, C.T., P.J. Coleman, Jr., B.R. Lichtenstein, and G. Schubert, The permanent and induced dipole moment of the moon, in Proceedings of the Fifth Lunar Science Conference, in press, 1974.

1-14. Russell, C.T., P.J. Coleman, Jr., and G. Schubert, Lunar magnetic field: Permanent and induced dipole moment, Science, in press, 1974.

1-15. Schubert, G., B.R. Lichtenstein, C.T. Russell, P.J. Coleman, Jr., B.F. Smith, D.S. Colburn, and C.P. Sonett, Lunar dayside plasma sheet depletion: Inference from magnetic observations, Geophysical Research Letters, in press, 1974.

1-16. Russell, C.T., P.J. Coleman, Jr., and G. Schubert, The lunar magnetic field, Space Research XV, in press, 1974.

1-17. Schubert, G. and B.R. Lichtenstein, Observations of Moon-plasma interactions by Explorer 35 and Apollo surface and orbital experiments, Rev. Geophys. Plan. Phys., in press, 1974.

1-18. Schubert, G. and B.R. Lichtenstein, A summary of "Observations moon-plasma interactions by Explorer 35 and Apollo surface and orbital experiments", in Solar Wind Three (ed. by C.T. Russell), in press, 1974.

2. Published papers in which the subsatellite data played a secondary but important role.

2-1. Anderson, K.A., L.M. Chase, R.P. Lin, J.E. McCoy and R.E. McGuire, Solar wind and interplanetary electron measurements on the Apollo 15 subsatellite, J. Geophys. Res., 77(25), 4611-4626, 1972.

2-2. Howe, H.C., R.P. Lin, R.E. McGuire and K.A. Anderson, Energetic electron scattering from the lunar remanent magnetic field, Geophysical Research Letters, 1, in press, 1974.

3. Papers presented at meetings in which the subsatellite data played a primary role.

3-1. Coleman, P.J., Jr., C.T. Russell and L.R. Sharp, Magnetic field measurements with the Apollo 15 subsatellite, presented at the Conference on Lunar Geophysics, The Lunar Science Institute, Houston, Texas, October 1971.

3-2. Coleman, P.J., Jr., C.T. Russell and L.R. Sharp, Magnetic field measurements with the Apollo 15 subsatellite, presented at 41st Annual International Meeting of the Society of Exploration Geophysicists, Houston, Texas, November 1971.

3-3. Coleman, P.J., Jr., L.R. Sharp, C.T. Russell and G. Schubert, Lunar limb effects in the solar wind, presented at the Fall American Geophysical Union Meeting, December, 1971 (abstract) EOS 52(11), 855, 1971.

3-4. Sharp, L.R., P.J. Coleman, Jr., C.T. Russell and G. Schubert, Lunar magcons, presented at the Fall American Geophysical Union Meeting, December 1971, (abstract), EOS 52(11), 857, 1971.

3-5. Coleman, P.J., Jr., C.T. Russell and L.R. Sharp, Magnetic field measurements with the Apollo 15 subsatellite, presented at the Apollo 15 Principal Investigators' Conference, Houston, Texas, December 1971.

3-6. Coleman, P.J., Jr., C.T. Russell, and L.R. Sharp, Magnetic fields near the moon, Third Lunar Science Conference, Houston, Texas, January, 1972.

3-7. Sharp, L.R., P.J. Coleman, Jr., C.T. Russell and G. Schubert, The magnetic field of the moon, presented at the Spring American Geophysical Union Meeting, (abstract), EOS 53(4), 441, 1972.

3-8. Russell, C.T., P.J. Coleman, Jr., B.R. Lichtenstein, G. Schubert and L.R. Sharp, Surface and orbital results from Apollo 15, presented at the XVth Plenary Meeting of COSPAR, Madrid, May, 1972.

3-9, Lichtenstein, B.R., C.T. Russell and P.J. Coleman, Jr., Magnetic measurements of the solar wind interaction with the moon, presented at Symposium on Photon and Particle Interactions with Surfaces in Space, Noordwijk, Holland, September, 1972.

3-10. Lichtenstein, B.R., C.T. Russell and P.J. Coleman, Jr., Measurements of the solar wind-moon interaction with the Apollo 15 and 16 subsatellite magnetometers, presented at the Fall American Geophysical Union Meeting (abstract), EOS 53(11), 1111, 1972.

3-11. Sharp, L.R., P.J. Coleman, Jr., and C.T. Russell, Lunar surface remanent magnetization as measured by the Apollo 15 and 16 subsatellite magnetometers, presented at the Fall American Geophysical Union Meeting (abstract), EOS 53(11), 1033, 1972.

3-12. Russell, C.T., P.J. Coleman, B.R. Lichtenstein, G. Schubert and L.R. Sharp, Lunar magnetic fields, presented at the Lunar Science Institute Conference on Geophysical and Geochemical Exploration of the Moon and Planets, Houston, Texas, January 1973.

3-13. Russell, C.T., P.J. Coleman, Jr., B.R. Lichtenstein, G. Schubert and L.R. Sharp, Apollo 15 and 16 subsatellite measurements of the lunar magnetic field, presented at the 4th Lunar Science Conference (abstract) Lunar Science IV (eds. J.W. Chamberlain and C. Watkins) Lunar Science Institute, 1973.

3-14. Schubert, G., B.R. Lichtenstein, P.J. Coleman, Jr., and C.T. Russell, Simultaneous observations of transient events by the Explorer 35 and Apollo 15 subsatellite magnetometers: Implications for lunar electrical conductivity studies, presented at Symposium on Inversion of Geophysical Data, University of Utah, Salt Lake City; March 1973.

3-15. Sharp, L.R., C.T. Russell, P.J. Coleman, Jr., The dipole field of the moon, presented at the Spring American Geophysical Union meeting (abstract) EOS 54(4), 358, 1973.

3-16. Lichtenstein, B.R., C.T. Russell, and P.J. Coleman, Jr., On the nature of lunar limb compressions, presented at the Spring American Geophysical Union Meeting, (abstract), EOS, 54(4), 443, 1973.

3-17. Sharp, L.R., P.J. Coleman, Jr., B.R. Lichtenstein, C.T. Russell and G. Schubert, Orbital mapping of the lunar magnetic field, presented at the Harold Urey Symposium on the Moon at the Lunar Science Institute, Houston, Texas, May, 1973.

3-18. Russell, C.T., P.J. Coleman, Jr., B.R. Lichtenstein, G. Schubert, and L.R. Sharp, Apollo 15 and 16 sub-satellite magnetometer measurements of the lunar magnetic field, presented at the XVIth Plenary Meeting of Cospar, Konstanz, Germany, June 1973.

3-19. Russell, C.T., Orbital magnetic surveys of the moon, presented at the annual meeting of the Geological Society of America, Dallas, Texas, November, 1973.

3-20. Russell, C.T., P.J. Coleman, Jr., B.R. Lichtenstein, and G. Schubert, Vector mapping of the lunar magnetic field, presented at Fall American Geophysical Union Meeting, (abstract), EOS Trans. AGU, 54(11), 1128, 1973.

3-21. Lichtenstein, B.R., G. Schubert, C.T. Russell, and P.J. Coleman, Jr., Magnetic field observations at low altitude over the moon, presented at the Fall American Geophysical Union meeting (abstract), EOS Trans. AGU, 54(11), 1195, 1973.

3-22. Russell, C.T., P.J. Coleman, Jr., B.R. Lichtenstein and G. Schubert, The permanent and induced magnetic dipole moment of the moon, presented at the Fifth Lunar Science Conference, Houston, Texas, March, 1974.

3-23. Russell, C.T., P.J. Coleman, Jr., B.R. Lichtenstein and G. Schubert, Fine scale mapping of the lunar magnetic field, presented at the 55th annual meeting of the American Geophysical Union, (abstract) EOS Trans. AGU, 55(4), 329, 1974.

3-24. Lichtenstein, B.R., C.T. Russell, P.J. Coleman, Jr., and G. Schubert, On the occurrence of compressional disturbances over the lunar limbs, presented at the 55th annual meeting of the American Geophysical Union (abstract), EOS Trans. AGU, 55(4), 413, 1974.

3-25. Russell, C.T., P.J. Coleman, Jr., G. Schubert, The lunar magnetic field, presented at the COSPAR XVIIth Plenary Meeting, Sao Paulo, Brazil, June, 1974.

4. Papers presented at meetings in which the subsatellite magnetometer data played a secondary but important role.

4-1. Anderson, K.A., L.M. Chase, R.P. Lin, J.E. McCoy and R.E. McGuire, Measurements of the solar wind cavity behind the moon from the Apollo 15 subsatellite, presented at the Fall American Geophysical Union Meeting, December 1971, (abstract), EOS 52(11), 910, 1971.

4-2. Fenner, M.A., J.W. Freeman, Jr., H.K. Hills, R.A. Lindeman, Magnetosheath structure observed by ALSEP/SIDE plasma detectors, presented at the Spring American Geophysical Union Meeting, April 1972, (abstract), EOS 53(4), 486, 1972.

4-3. Chase, L.M., Plasmasheet observations at lunar orbit, presented at the Conference on Magnetospheric Substorms, Rice University, October, 1972.

4-4. Chase, L.M., Particle characteristics in the earth's magnetotail at 60 Re, presented at the Fall American Geophysical Union Meeting, December 1972 (abstract) EOS, 53(11), 1101, 1972.

4-5. McGuire, R.E., K.A. Anderson, L.M. Chase, R.P. Lin, J.E. McCoy, Particle observations during the passage of the interplanetary shock of May 15, 1972, presented at the Fall American Geophysical Union Meeting December 1972 (abstract), EOS 53(11), 1086, 1972.

4-6. Bratenahl, A., B.E. Goldstein, D.R. Clay, and M. Neugebauer, Correlated field and plasma flow characteristics at the lunar-distant magnetopause, presented at the Fall American Geophysical Union Meeting, (abstract), EOS Trans. AGU, 54(11), 1196, 1973.

4-7. Anderson, K.A., H.C. Howe, R.P. Lin, R.E. McGuire, L.M. Chase and J.E. McCoy, Observation of energetic electron mirroring from the lunar remnant magnetic field, presented at the 5th Lunar Science Conference (abstract), Lunar Science V, Lunar Science Institute, p. 18, 1974.

4-8. Howe, H.C., K.A. Anderson, R.P. Lin, R.E. McGuire and J.E. McCoy, Energetic electron mirroring from the lunar remnant magnetic field, presented at the 55th Annual American Geophysical Union Meeting (abstract), EOS Trans. AGU, 55(4), 391, 1974.